A Poisson multi-Bernoulli mixture filter for coexisting point and extended targets

Ángel F. García-Fernández, Jason L. Williams, Lennart Svensson, Yuxuan Xia

***Abstract*—This paper proposes a Poisson multi-Bernoulli mixture (PMBM) filter for coexisting point and extended targets, i.e., for scenarios where there may be simultaneous point and extended targets. The PMBM filter provides a recursion to compute the multi-target filtering posterior based on probabilistic information on data associations, and single-target predictions and updates. In this paper, we first derive the PMBM filter update for a generalised measurement model, which can include measurements originated from point and extended targets. Second, we propose a single-target space that accommodates both point and extended targets and derive the filtering recursion that propagates Gaussian densities for point targets and gamma Gaussian inverse Wishart densities for extended targets. As a computationally efficient approximation of the PMBM filter, we also develop a Poisson multi-Bernoulli (PMB) filter for coexisting point and extended targets. The resulting filters are analysed via numerical simulations.**

***Index Terms*—Multiple target filtering, point targets, extended targets.**

I. Introduction

Multiple target filtering refers to the sequential estimation of the states of the current targets, which may appear, move and disappear, given past and current noisy sensor measurements. This is a key component in many applications such as self-driving vehicles [1] and maritime navigation [2]. Multi-target filtering can be solved in a Bayesian framework by computing the posterior density on the current set of targets, given probabilistic models for target births, dynamics and deaths, and also models for the measurements, obtained from one or multiple sensors [3], [4]. The target birth model contains probabilistic information on where targets may appear in the surveillance area, and it enables the resulting filters to contain information on potential targets that may remain occluded [5, Fig. 6], which is of paramount importance in some applications such as self-driving vehicles.

If the target extent is small compared to the sensor resolution, it is common to use point-target modelling. In this model, a target state typically contains kinematic information, such as position and velocity, and one target can generate at most one measurement at each time step [6]. Conversely, if the target extent is large compared to the sensor resolution, a better choice is to use extended target modelling [7]. Here, the target state usually contains both kinematic information and information on its extent, e.g., represented by an ellipse [8]. In addition, each extended target may generate more than one measurement at each time step, represented via a Poisson point process (PPP) in the standard model [7], [9], [10].

For both point and extended targets with Poisson birth model and the standard measurement models, the posterior density is a Poisson multi-Bernoulli mixture (PMBM), which can be calculated by the corresponding PMBM filtering recursions[1] [5], [11], [12]. The PMBM has a compact representation of global hypotheses, representing undetected targets via the intensity of a PPP and making use of probabilistic target existence in each global hypothesis. The PMBM recursion can also handle a multi-Bernoulli birth model by setting the PPP intensity to zero and adding new Bernoulli components in the prediction step, resulting in the MBM filter [12], [13]. The MBM filter can also be extended to consider multi-Bernoullis with deterministic target existence, which we refer to as the MBM_{01} filter, at the expense of increasing the number of global hypotheses [12, Sec. IV]. Both MBM and MBM_{01} filters can consider target states with labels, and the (labelled) MBM_{01} filtering recursion is analogous to the δ-generalised labelled multi-Bernoulli (δ-GLMB) filter [14], [15].

There are applications in which it is important to have more general models than the standard point and extended target models [3]. Specifically, there may be some targets that are small compared to the sensor resolution, while other targets are large, which implies that there are coexisting point/extended targets in the field of view. For example, in a self-driving vehicle application, pedestrians may be modelled as point targets while other vehicles as extended targets. The distinction between point and extended targets may also depend on the distance, as sensor resolution is usually higher at short distances. Therefore, it is of interest to develop multi-target filters that can handle coexisting point and extended targets. The extended target measurement models in [15], [16] are general enough to model measurements from coexisting point and extended targets, but no single-target state, dynamic model and filter implementations are presented for this case.

In this paper, we fill this gap and propose a PMBM filter for coexisting point and extended targets. In order to do so, we first develop a PMBM filtering recursion for a generalised measurement model, in which each target generates an inde-

A. F. García-Fernández is with the Department of Electrical Engineering and Electronics, University of Liverpool, Liverpool L69 3GJ, United Kingdom (angel.garcia-fernandez@liverpool.ac.uk). He is also with the ARIES Research Centre, Universidad Antonio de Nebrija, Madrid, Spain. J. L. Williams is with the Commonwealth Scientific and Industrial Research Organization (jason.williams@data61.csiro.au). L. Svensson and Y. Xia are with the Department of Electrical Engineering, Chalmers University of Technology, SE-412 96 Gothenburg, Sweden (firstname.lastname@chalmers.se).

This paper has supplementary downloadable material available at http://ieeexplore.ieee.org., provided by the authors. The material includes the appendices. This material is 268KB in size.

[1] A course on multiple target tracking with detailed information on these topics can be found at https://www.youtube.com/channel/UCa2-fpj6AV8T6JK1uTRuFpw.

pendent set of measurements with an arbitrary distribution, and clutter is a PPP. With a suitable choice of the target-generated measurement distribution, this generalised model recovers the standard point and extended target measurement models. As a result, the PMBM filter with the generalised measurement model can be used to address multi-target filtering problems with point and extended targets [5], [11], [12], and more general problems. For example, the generalised measurement model can also be used for diffuse multipath [17], extended targets composed of point-scatterers [7], and point targets with stationary landmarks, modelled as extended targets. The resulting PMBM recursion has a track-oriented form that enables efficient implementation [18].

Based on the developed PMBM filtering recursion, the second contribution is to derive a PMBM filter for coexisting point and extended targets. In this setting, each Bernoulli contains probabilistic information on target existence and type, either point or extended target. The implementation is provided for a linear Gaussian model for point targets [19] and a Gamma Gaussian Inverse Wishart (GGIW) model for extended targets [5], [7], [20]. Finally, we explain how a PMBM density in this context can be projected onto a Poisson multi-Bernoulli (PMB) density [11]. Performing this projection after each update provides us with a PMB filter, which is a fast approximation to the PMBM filter. Simulation results are provided to analyse the performance of the filters.

The rest of the paper is organised as follows. Section II introduces the problem formulation and an overview of the solution. The update for the PMBM filter with generalised measurement model is derived in Section III. Section IV explains the PMBM filter for coexisting point and extended targets, and the PMB projection. Simulation results and conclusions are given in Sections V and VI, respectively.

II. Problem formulation and overview of the solution

This paper deals with multiple target tracking with both point and extended target models. This section presents an overview of a PMBM filter with a generalised measurement model that will be used to model coexisting point and extended targets in Section IV. We introduce the models in Section II-A and the PMBM filter overview in Section II-B.

A. Models

A single target state $x \in \mathcal{X}$, where $\mathcal{X}$ is a locally compact, Hausdorff and second-countable (LCHS) space [3], contains the information of interest about the target, for example, its position, velocity and extent. The set of targets at time k is denoted by $X_k \in \mathcal{F}(\mathcal{X})$, where $\mathcal{F}(\mathcal{X})$ represents the set of finite subsets of $\mathcal{X}$.

A main novelty in this paper is the development of a PMBM filter with a generalised measurement model. Here, the set X_k of targets at time step k, is observed through a set $Z_k \in \mathcal{F}(\mathbb{R}^{n_z})$ of noisy measurements, which consist of the union of target-generated measurements and clutter, with the model:

- Each target $x \in X_k$ generates an independent set Z of measurements with density $f(Z|x)$.
- Clutter is a PPP with intensity $\lambda^C(\cdot)$.

It should be noted that the standard point and extended measurement models [5], [11] can be recovered by suitable choices of $f(Z|x)$.

We also consider the standard dynamic model for targets. Given the set X_k of targets at time step k, each target $x \in X_k$ survives with probability $p^S(x)$ and moves to a new state with a transition density $g(\cdot|x)$, or dies with probability $1-p^S(x)$. At time step k, targets are born independently following a Poisson point process (PPP) with intensity $\lambda_k^B(\cdot)$.

B. PMBM posterior

In this paper, we show that, for the above-mentioned measurement and dynamic models, the density $f_{k|k'}(\cdot)$ of X_k given the sequence of measurements $(Z_1, ..., Z_{k'})$, where $k' \in \{k-1, k\}$, is a PMBM density. This section provides an overview of the PMBM posterior and its data association hypotheses.

The PMBM is of the form [11], [12]

$$f_{k|k'}(X_k) = \sum_{Y \uplus W = X_k} f^{\mathrm{p}}_{k|k'}(Y) f^{\mathrm{mbm}}_{k|k'}(W) \tag{1}$$

$$f^{\mathrm{p}}_{k|k'}(X_k) = e^{-\int \lambda_{k|k'}(x)dx} \prod_{x \in X_k} \lambda_{k|k'}(x) \tag{2}$$

$$f^{\mathrm{mbm}}_{k|k'}(X_k) = \sum_{a \in \mathcal{A}_{k|k'}} w^a_{k|k'} \sum_{\uplus_{l=1}^{n_{k|k'}} X^l = X_k} \prod_{i=1}^{n_{k|k'}} f^{i,a^i}_{k|k'}\left(X^i\right) \tag{3}$$

where $\lambda_{k|k'}(\cdot)$ is the intensity of the PPP $f^{\mathrm{p}}_{k|k'}(\cdot)$, representing undetected targets, and $f^{\mathrm{mbm}}_{k|k'}(\cdot)$ is a multi-Bernoulli mixture representing potential targets that have been detected at some point up to time step k'. Symbol $\uplus$ denotes the disjoint union and the summation in (1) is taken over all mutually disjoint (and possibly empty) sets Y and W whose union is X_k, i.e., X_k is fixed, and Y and W free.

In the PMBM posterior, there are $n_{k|k'}$ Bernoulli components and for each Bernoulli there are $h^i_{k|k'}$ possible local hypotheses. By selecting a local hypothesis $a^i \in \left\{1, ..., h^i_{k|k'}\right\}$ for each Bernoulli, we obtain a global hypothesis $a = \left(a^1, ..., a^{n_{k|k'}}\right) \in \mathcal{A}_{k|k'}$, where $\mathcal{A}_{k|k'}$ is the set of global hypotheses. Each global hypothesis represents a multi-Bernoulli distribution. The i-th Bernoulli component with local hypothesis a^i has a density

$$f^{i,a^i}_{k|k'}(X) = \begin{cases} 1 - r^{i,a^i}_{k|k'} & X = \emptyset \\ r^{i,a^i}_{k|k'} f^{i,a^i}_{k|k'}(x) & X = \{x\} \\ 0 & \text{otherwise} \end{cases} \tag{4}$$

where $r^{i,a^i}_{k|k'}$ is the probability of existence and $f^{i,a^i}_{k|k'}(x)$ the single target density. The weight of global hypothesis a is $w^a_{k|k'}$ and meets

$$w^a_{k|k'} \propto \prod_{i=1}^{n_{k|k'}} w^{i,a^i}_{k|k'} \tag{5}$$

where $w^{i,a^i}_{k|k'}$ is the weight of the i-th Bernoulli with local hypothesis a^i, and $\sum_{a \in \mathcal{A}_{k|k'}} w^a_{k|k'} = 1$.

The set of feasible global hypotheses is defined as in the extended target case [5], [21]. We denote the measurement set at time step k as $Z_k = \left\{z_k^1, ..., z_k^{m_k}\right\}$. We refer to measurement z_k^j using the pair (k, j) and the set of all such measurement pairs up to (and including) time step k is denoted by $\mathcal{M}_k$. Then, a single target hypothesis a^i for the i-th Bernoulli component has a set of measurement pairs denoted as $\mathcal{M}_k^{i,a^i} \subseteq \mathcal{M}_k$. The set $\mathcal{A}_{k|k'}$ of all global hypotheses meets

$$\mathcal{A}_{k|k'} = \Bigg\{ \left(a^1, ..., a^{n_{k|k'}}\right) : a^i \in \left\{1, ..., h_{k|k'}^i\right\} \forall i, \bigcup_{i=1}^{n_{k|k'}} \mathcal{M}_{k'}^{i,a^i} = \mathcal{M}_{k'}, \mathcal{M}_{k'}^{i,a^i} \cap \mathcal{M}_{k'}^{j,a^j} = \emptyset, \forall i \neq j \Bigg\}.$$

That is, all measurements must be assigned to a local hypothesis, and there cannot be more than one local hypothesis with the same measurement. More than one measurement can be associated to the same local hypothesis at the same time step. Each global hypothesis therefore corresponds to a unique partition of $\mathcal{M}_{k'}$ [5, Sec. V], and the number of global hypothesis is the Bell number of $|\mathcal{M}_{k'}|$. At each time step, each non-empty subset of Z_k generates a new Bernoulli component, corresponding to a potential target detected for the first time or clutter. This implies that, at each time step, $2^{m_k} - 1$ new Bernoulli components are generated.

It should be noted that the prediction step of a PMBM density is closed-form for the standard dynamic models [11], [12], and is not affected by the choice of measurement model. Therefore, the next section focuses on the update and we omit the details for prediction, which can be found in [11], [12].

III. PMBM UPDATE FOR A GENERALISED MEASUREMENT MODEL

This section provides the PMBM filter update step with the measurement model in Section II. We denote a Kronecker delta as $\delta_i[\cdot]$, with $\delta_i[u] = 1$ if $u = i$ and $\delta_i[u] = 0$, otherwise. Also, given two real-valued functions $a(\cdot)$ and $b(\cdot)$ on the target space, we denote their inner product as

$$\langle a, b \rangle = \int a(x)\, b(x)\, dx. \tag{6}$$

A. Update

The update of the predicted PMBM $f_{k|k-1}(\cdot)$ after observing Z_k is given in the following theorem.

Theorem 1. *Assume the predicted density $f_{k|k-1}(\cdot)$ is a PMBM of the form (1). Then, the updated density $f_{k|k}(\cdot)$ with set $Z_k = \left\{z_k^1, ..., z_k^{m_k}\right\}$ is a PMBM with the following parameters. The number of Bernoulli components is $n_{k|k} = n_{k|k-1} + 2^{m_k}$. The intensity of the PPP is*

$$\lambda_{k|k}(x) = f(\emptyset|x)\, \lambda_{k|k-1}(x). \tag{7}$$

For Bernoullis continuing from previous time steps $i \in \left\{1, ..., n_{k|k-1}\right\}$, a new local hypothesis is included for each previous local hypothesis and either a misdetection or an update with a non-empty subset of Z_k. The updated number of local hypotheses is $h_{k|k}^i = 2^{m_k} h_{k|k-1}^i$. For missed detection hypotheses, $i \in \left\{1, ..., n_{k|k-1}\right\}$, $a^i \in \left\{1, ..., h_{k|k-1}^i\right\}$, we obtain

$$\mathcal{M}_k^{i,a^i} = \mathcal{M}_{k-1}^{i,a^i} \tag{8}$$

$$l_{k|k}^{i,a^i,\emptyset} = \left\langle f_{k|k-1}^{i,a^i}, f(\emptyset|\cdot) \right\rangle \tag{9}$$

$$w_{k|k}^{i,a^i} = w_{k|k-1}^{i,a^i} \left[1 - r_{k|k-1}^{i,a^i} + r_{k|k-1}^{i,a^i} l_{k|k}^{i,a^i,\emptyset}\right] \tag{10}$$

$$r_{k|k}^{i,a^i} = \frac{r_{k|k-1}^{i,a^i} l_{k|k}^{i,a^i,\emptyset}}{1 - r_{k|k-1}^{i,a^i} + r_{k|k-1}^{i,a^i} l_{k|k}^{i,a^i,\emptyset}} \tag{11}$$

$$f_{k|k}^{i,a^i}(x) = \frac{f(\emptyset|x)\, f_{k|k-1}^{i,a^i}(x)}{l_{k|k}^{i,a^i,\emptyset}}. \tag{12}$$

Let $Z_k^1, ..., Z_k^{2^{m_k}-1}$ be the nonempty subsets of Z_k. For a Bernoulli $i \in \left\{1, ..., n_{k|k-1}\right\}$ with a single target hypothesis $\widetilde{a}^i \in \left\{1, ..., h_{k|k-1}^i\right\}$ in the predicted density, the new local hypothesis generated by a set Z_k^j has $a^i = \widetilde{a}^i + h_{k|k-1}^i j$, $r_{k|k}^{i,a^i} = 1$, and

$$\mathcal{M}_k^{i,a^i} = \mathcal{M}_{k-1}^{i,\widetilde{a}^i} \cup \left\{(k,p) : z_k^p \in Z_k^j\right\} \tag{13}$$

$$l_{k|k}^{i,a^i,Z_k^j} = \left\langle f_{k|k-1}^{i,\widetilde{a}^i}, f\left(Z_k^j|\cdot\right) \right\rangle \tag{14}$$

$$w_{k|k}^{i,a^i} = w_{k|k-1}^{i,\widetilde{a}^i} r_{k|k-1}^{i,\widetilde{a}^i} l_{k|k}^{i,a^i,Z_k^j} \tag{15}$$

$$f_{k|k}^{i,a^i}(x) = \frac{f\left(Z_k^j|x\right) f_{k|k-1}^{i,\widetilde{a}^i}(x)}{l_{k|k}^{i,a^i,Z_k^j}}. \tag{16}$$

For the new Bernoulli initiated by subset Z_k^j, whose index is $i = n_{k|k-1} + j$, we have two single target hypotheses ($h_{k|k}^i = 2$), one corresponding to a non-existent Bernoulli

$$\mathcal{M}_k^{i,1} = \emptyset,\ w_{k|k}^{i,1} = 1,\ r_{k|k}^{i,1} = 0 \tag{17}$$

and the other

$$\mathcal{M}_k^{i,2} = \left\{(k,p) : z_k^p \in Z_k^j\right\} \tag{18}$$

$$l_{k|k}^{Z_k^j} = \left\langle \lambda_{k|k-1}, f\left(Z_k^j|\cdot\right) \right\rangle \tag{19}$$

$$w_{k|k}^{i,2} = \delta_1\left[|Z_k^j|\right] \left[\prod_{z \in Z_k^j} \lambda^C(z)\right] + l_{k|k}^{Z_k^j} \tag{20}$$

$$r_{k|k}^{i,2} = \frac{l_{k|k}^{Z_k^j}}{w_{k|k}^{i,a^i}} \tag{21}$$

$$f_{k|k}^{i,2}(x) = \frac{f\left(Z_k^j|x\right) \lambda_{k|k-1}(x)}{l_{k|k}^{Z_k^j}}. \quad \square \tag{22}$$

Theorem 1 is proved in Appendix A. We can see that the updated PPP intensity in (7) corresponds to the predicted intensity multiplied by the probability of not receiving any measurements. This is expected as the PPP contains information on the undetected targets. Misdetection hypotheses lower the probability of existence of the Bernoullis via (9) and (11).

If $f(\emptyset|x)$ does not depend on x, the single-target densities of misdetection hypotheses remain unchanged, see (12).

For the update of a previous Bernoulli component with subset Z_k^j, the updated Bernoulli has a probability of existence equal to one. Each non-empty subset $Z_k^j \subseteq Z_k$ creates a new Bernoulli component. If $|Z_k^j| > 1$, the existence probability $r_{k|k}^{i,2}$ of the new Bernoulli component is one, which implies that, conditioned on the corresponding hypothesis, this Bernoulli represents an existing target. If $|Z_k^j| = 1$, the existence probability $r_{k|k}^{i,2}$ of the new Bernoulli component depends on the clutter intensity $\lambda^C(\cdot)$, as this Bernoulli may correspond to a target or to clutter. The higher $\lambda^C(\cdot)$, the lower the probability of existence of this potential target.

B. Relation to standard point/extended target models

In the standard point target measurement model, a target x is detected with probability $p^D(x)$ and, if detected, it generates one measurement with density $l(\cdot|x)$. This model is obtained by setting

$$f(Z|x) = \begin{cases} 1 - p^D(x) & Z = \emptyset \\ p^D(x)\, l(z|x) & Z = \{z\} \\ 0 & |Z| > 1. \end{cases} \tag{23}$$

If we use the above definitions of local and global hypotheses and Theorem 1 for point targets, many of the global hypotheses contain local hypotheses where more than one measurement is associated to the same Bernoulli at the same time step. Since this is impossible according to (23), all these hypotheses would obtain weight zero. A more convenient way to handle point targets is to exclude these hypotheses from the set $\mathcal{A}_{k|k}$ that we consider, see [11].

In the standard extended target model, a target x is detected with probability $p^D(x)$ and, if detected, it generates a PPP measurement with intensity $\gamma(x)\, l(\cdot|x)$, where $l(\cdot|x)$ is a single-measurement density and $\gamma(x)$ is the expected number of measurements. We can recover this model by setting

$$f(Z|x) = \begin{cases} 1 - p^D(x) + p^D(x)\, e^{-\gamma(x)} & Z = \emptyset \\ p^D(x)\, \gamma^{|Z|}(x)\, e^{-\gamma(x)} \prod_{z \in Z} l(z|x) & |Z| > 0. \end{cases} \tag{24}$$

In this case, Theorem 1 becomes the standard extended-target PMBM update in track-oriented form [5], [21].

C. Discussion

We have shown that the update of a PMBM prior with the generalised measurement model in Section II is also PMBM. The proposed measurement model contains the standard point target and extended target measurement models as particular cases, and can be used for other types of measurement modelling. For example, another important special case is that each target could generate a union of independent Bernoulli measurements, which can model extended targets that consist of reflection points [22], [23]. It can also model extended targets with binomially distributed target-generated measurements [24]. The considered measurement model also allows us to model coexisting point and extended targets, for example, modelling radar returns from vehicles (extended targets) and pedestrians (point targets), as will be explained in Section IV. It can also model scenarios in which far-away targets produce point-target measurements and targets that are sufficiently close produce extended-target measurements, for example, by setting a distance threshold, which may depend on the target extent, to switch between both types of model. The proposed PMBM update requires PPP clutter, which can be relaxed in Bernoulli filters [25].

We would also like to remark that we have presented the results for PPP birth density, as we think this is generally the most suitable birth process, due to the lower number of generated hypotheses [12], [13]. Nevertheless, the presented results also hold for the following cases. For multi-Bernoulli birth, the above equations are valid, by setting the Poisson intensity equal to zero, and adding the Bernoulli components for new born targets in the prediction step [12], [13]. In this case, the posterior is a multi-Bernoulli mixture (MBM), which can also be represented as MBM_{01} [12, Sec. IV]. For multi-Bernoulli birth, one can also uniquely label each Bernoulli component, for which the labelled MBM_{01} recursion would correspond to the δ-GLMB filter recursion [15].

IV. PMBM filter for coexisting point and extended targets

This section presents the PMBM filter, and a track-oriented PMB filter, for coexisting point and extended targets. The single target space for point targets is $\mathbb{R}^{n_x}$, which represents the kinematic state (e.g. position and velocity). We model extended targets with the GGIW model [16], whose space is $\mathcal{X}_e = \mathbb{R}_+ \times \mathbb{R}^{n_x} \times \mathbb{S}_+^d$, where $\mathbb{R}_+$ represents the positive real numbers and $\mathbb{S}_+^d$ the positive definite matrices of size d, which is the dimension of the extent.

The single target space for coexisting point/extended targets is then $\mathcal{X} = \mathbb{R}^{n_x} \uplus \mathcal{X}_e$, where $\uplus$ stands for union of sets that are mutually disjoint, i.e., $\mathcal{X} = \mathbb{R}^{n_x} \cup \mathcal{X}_e$ and $\mathbb{R}^{n_x} \cap \mathcal{X}_e = \emptyset$ [3]. Other works with this type of hybrid space are for example [3], [26]–[28]. If $x \in \mathcal{X}_e$, then $x = (\gamma, \xi, X)$, where γ represents the expected number of measurements per target, ξ is the kinematic state and X is the extent state that describes the target's size and shape. It should be noted that, though not necessary, it is also possible to include a class variable in the target space to distinguish between point and extended targets, as in interacting multiple models [29], see Appendix B. This appendix also explains the corresponding single-target integral.

We use a measurement model that corresponds to the standard point and extended target measurement models depending on the type of target we observe. That is, for $x \in \mathbb{R}^{n_x}$, $f(Z|x)$ is given by (23) with a probability $p^D(x) = p_1^D$ of detection, $l(z|x) = \mathcal{N}(z; H_1 x, R)$ where H_1 is the measurement matrix, R is the noise covariance matrix, and $\mathcal{N}(\cdot; \overline{x}, P)$ is a Gaussian density with mean $\overline{x}$ and covariance P. For $x \in \mathcal{X}_e$, $f(Z|x)$ is given by (24) with a probability $p^D(x) = p_2^D$ of detection, $\gamma(x) = \gamma$, and $l(z|x) = \mathcal{N}(z; H_2 \xi, X)$ where H_2 is the measurement matrix.

The rest of this section is organised as follows. Section IV-A presents the considered single-target densities. The update and the prediction are provided in Sections IV-B and IV-C. The PMB approximation is addressed in Section IV-D. Target state estimation is explained in Section IV-E. Practical aspects are discussed in Section IV-F.

A. Single-target densities

We develop a PMBM implementation in which we propagate a Gaussian for single target densities and a (factorised) GGIW density for extended target densities [7], [20], [30]. In a factorised GGIW density, the distributions for γ, ξ and X are independent, which has computational and practical benefits [7, Sec. III.A.2].

The Gaussian density for $x \in \mathcal{X}$ with mean $\overline{x}^{i,a^i,1}_{k|k'}$ and covariance matrix $P^{i,a^i,1}_{k|k'}$ is

$$\mathcal{N}_p\left(x; \overline{x}^{i,a^i,1}_{k|k'}, P^{i,a^i,1}_{k|k'}\right) = \mathcal{N}\left(x; \overline{x}^{i,a^i,1}_{k|k'}, P^{i,a^i,1}_{k|k'}\right) \tag{25}$$

for $x \in \mathbb{R}^{n_x}$ and zero for $x \in \mathcal{X}_e$. Note that $\mathcal{N}_p(\cdot)$ is zero evaluated at $x \in \mathcal{X}_e$, as $\mathcal{N}_p(\cdot)$ represents point targets.

The Gamma density with parameters $\alpha > 0$ and $\beta > 0$ is denoted as $\mathcal{G}(\cdot; \alpha, \beta)$. The inverse Wishart density on matrices in $\mathbb{S}^d_+$ with $v > 2d$ degrees of freedom and parameter matrix $V \in \mathbb{S}^d_+$ is denoted as $\mathcal{IW}(\cdot; v, V)$ [31]. Then, the GGIW density for $x \in \mathcal{X}$ with parameters

$$\zeta^{i,a^i}_{k|k'} = \left(\alpha^{i,a^i}_{k|k'}, \beta^{i,a^i}_{k|k'}, \overline{x}^{i,a^i,2}_{k|k'}, P^{i,a^i,2}_{k|k'}, v^{i,a^i}_{k|k'}, V^{i,a^i}_{k|k'}\right) \tag{26}$$

is

$$\begin{aligned}\mathcal{G}_e\left(x; \zeta^{i,a^i}_{k|k'}\right) = \mathcal{G}\left(\gamma; \alpha^{i,a^i}_{k|k'}, \beta^{i,a^i}_{k|k'}\right) \mathcal{N}\left(\xi; \overline{x}^{i,a^i,2}_{k|k'}, P^{i,a^i,2}_{k|k'}\right) \\ \times \mathcal{IW}\left(X; v^{i,a^i}_{k|k'}, V^{i,a^i}_{k|k'}\right)\end{aligned} \tag{27}$$

for $x \in \mathcal{X}_e$ and zero for $x \in \mathbb{R}^{n_x}$.

The single-target density of the i-th Bernoulli and local hypothesis a^i is

$$\begin{aligned}f^{i,a^i}_{k|k'}(x) = c^{i,a^i}_{k|k'} \mathcal{N}_p\left(x; \overline{x}^{i,a^i,1}_{k|k'}, P^{i,a^i,1}_{k|k'}\right) \\ + \left(1 - c^{i,a^i}_{k|k'}\right) \mathcal{G}_e\left(x; \zeta^{i,a^i}_{k|k'}\right)\end{aligned} \tag{28}$$

where $c^{i,a^i}_{k|k'}$ and $\left(1 - c^{i,a^i}_{k|k'}\right)$ are the probabilities that the target is a point-target and and extended target, respectively. The PPP intensity is a mixture

$$\begin{aligned}\lambda_{k|k'}(x) = \sum_{q=1}^{n^p_{k|k'}} w^{p,q}_{k|k'} \mathcal{N}_p\left(x; \overline{x}^{p,q,1}_{k|k'}, P^{p,q,1}_{k|k'}\right) \\ + \sum_{q=1}^{n^e_{k|k'}} w^{e,q}_{k|k'} \mathcal{G}_e\left(x; \zeta^{e,q}_{k|k'}\right)\end{aligned} \tag{29}$$

where $n^p_{k|k'}$ is the number of components with point-targets, with weight $w^{p,q}_{k|k'}$, mean $\overline{x}^{p,q,1}_{k|k'}$ and covariance $P^{p,q,1}_{k|k'}$, and $n^e_{k|k'}$ is the number of components with extended targets, with weight $w^{e,q}_{k|k'}$ and parameters $\zeta^{e,q}_{k|k'}$. It should be noted that $\sum_{q=1}^{n^p_{k|k'}} w^{p,q}_{k|k'}$ and $\sum_{q=1}^{n^e_{k|k'}} w^{e,q}_{k|k'}$ represent the expected number of undetected point and extended targets, respectively.

B. Update

We represent the update of a GGIW density with parameters $\zeta^{i,a^i}_{k|k-1}$ with a given measurement set Z^j_k as a function

$$\left(\zeta^{e,q}_{k|k}, \ell^{e,q}_{k|k}\right) = \mathrm{u}_e\left(\zeta^{i,a^i}_{k|k-1}, Z^j_k\right)$$

where $\zeta^{e,q}_{k|k}$ is the updated GGIW and $\ell^{e,q}_{k|k}$ the marginal likelihood, see Appendix C. The Kalman filter update of a Gaussian density with mean $\overline{x}^{i,a^i,1}_{k|k-1}$ and covariance $P^{i,a^i,1}_{k|k-1}$ and measurement z is represented as

$$\left(\overline{x}^{i,a^i,1}_{k|k}, P^{i,a^i,1}_{k|k}, \ell^{i,a^i,1}_{k|k}\right) = \mathrm{u}_p\left(\overline{x}^{i,a^i,1}_{k|k-1}, P^{i,a^i,1}_{k|k-1}, z\right)$$

where $\overline{x}^{i,a^i,1}_{k|k}$ and $P^{i,a^i,1}_{k|k}$ are the updated mean and covariance, and $\ell^{i,a^i,1}_{k|k}$ is the marginal likelihood, see [19] for details.

We apply Theorem 1 to obtain the specific parameters of the updated PMBM provided in the following lemma.

Lemma 2. *The updated PMBM with a prior PMBM described by* (1), (28) *and* (29)*, with measurement set* $Z_k = \left\{z^1_k, ..., z^{m_k}_k\right\}$ *has the structure in Theorem 1 with the following parameters. The number of PPP components is* $n^p_{k|k} = n^p_{k|k-1}$ *and* $n^e_{k|k} = 2n^e_{k|k-1}$*. For point targets,*

$$\overline{x}^{p,q,1}_{k|k} = \overline{x}^{p,q,1}_{k|k-1}, P^{p,q,1}_{k|k} = P^{p,q,1}_{k|k-1}, \tag{30}$$

$$w^{p,q}_{k|k} = \left(1 - p^D_1\right) w^{p,q}_{k|k-1}. \tag{31}$$

For extended targets and $q \leq n^e_{k|k-1}$*, we have*

$$\zeta^{e,q}_{k|k} = \zeta^{e,q}_{k|k-1}, w^{e,q}_{k|k} = \left(1 - p^D_2\right) w^{e,q}_{k|k-1}. \tag{32}$$

For $q > n^e_{k|k-1}$, $\tilde{q} = q - n^e_{k|k-1}$,

$$\left(\zeta^{e,q}_{k|k}, \ell^{e,q}_{k|k}\right) = \mathrm{u}_e\left(\zeta^{e,\tilde{q}}_{k|k-1}, \emptyset\right) \tag{33}$$

$$w^{e,q}_{k|k} = p^D_2 \ell^{e,q}_{k|k} w^{e,\tilde{q}}_{k|k}. \tag{34}$$

For missed detection hypotheses of previous Bernoullis,

$$\begin{aligned}f^{i,a^i}_{k|k}(x) = c^{i,a^i}_{k|k} \mathcal{N}_p\left(x; \overline{x}^{i,a^i,1}_{k|k}, P^{i,a^i,1}_{k|k}\right) + \left(1 - c^{i,a^i}_{k|k}\right) \\ \times \left[w \mathcal{G}_e\left(x; \zeta^{i,a^i,1}_{k|k}\right) + (1 - w) \mathcal{G}_e\left(x; \zeta^{i,a^i,2}_{k|k}\right)\right]\end{aligned} \tag{35}$$

where $\overline{x}^{i,a^i,1}_{k|k} = \overline{x}^{i,a^i,1}_{k|k-1}$, $P^{i,a^i,1}_{k|k} = P^{i,a^i,1}_{k|k-1}$, $\zeta^{i,a^i,1}_{k|k} = \zeta^{i,a^i}_{k|k-1}$ *and*

$$\left(\zeta^{i,a^i,2}_{k|k}, \ell^{i,a^i,2}_{k|k}\right) = \mathrm{u}_e\left(\zeta^{i,a^i}_{k|k-1}, \emptyset\right) \tag{36}$$

$$\begin{aligned}l^{i,a^i,\emptyset}_{k|k} = c^{i,a^i}_{k|k-1}\left(1 - p^D_1\right) \\ + \left(1 - c^{i,a^i}_{k|k-1}\right)\left(1 - p^D_2 + p^D_2 \ell^{i,a^i,2}_{k|k}\right)\end{aligned} \tag{37}$$

$$w^{i,a^i}_{k|k} = w^{i,a^i}_{k|k-1}\left[1 - r^{i,a^i}_{k|k-1} + r^{i,a^i}_{k|k-1} l^{i,a^i,\emptyset}_{k|k}\right] \tag{38}$$

$$r^{i,a^i}_{k|k} = \frac{r^{i,a^i}_{k|k-1} l^{i,a^i,\emptyset}_{k|k}}{1 - r^{i,a^i}_{k|k-1} + r^{i,a^i}_{k|k-1} l^{i,a^i,\emptyset}_{k|k}} \tag{39}$$

$$c^{i,a^i}_{k|k} = \frac{\left(1 - p^D_1\right) c^{i,a^i}_{k|k-1}}{l^{i,a^i,\emptyset}_{k|k}} \tag{40}$$

$$w = \frac{1 - p_2^D}{1 - p_2^D + p_2^D \ell_{k|k}^{i,a^i,2}}. \tag{41}$$

The detection hypotheses of a previous Bernoulli with a subset Z_k^j*, with* $\left|Z_k^j\right| = m_k^j$*, has* $r_{k|k}^{i,a^i} = 1$*, and*

$$w_{k|k}^{i,a^i} = w_{k|k-1}^{i,\widetilde{a}^i} r_{k|k-1}^{i,\widetilde{a}^i} l_{k|k}^{i,a^i,Z_k^j} \tag{42}$$

$$\left(\zeta_{k|k}^{i,a^i}, \ell_{k|k}^{i,a^i}\right) = \mathrm{u}_e\left(\zeta_{k|k-1}^{i,\widetilde{a}^i}, Z_k^j\right). \tag{43}$$

For $m_k^j > 1$*,* $l_{k|k}^{i,a^i,Z_k^j} = p_2^D \ell_{k|k}^{i,a^i}$ *and* $c_{k|k}^{i,a^i} = 0$*, which implies that* $\overline{x}_{k|k}^{i,a^i,1}$ *and* $P_{k|k}^{i,a^i,1}$ *are irrelevant. For* $m_k^j = 1$*,* $Z_k^j = \{z\}$*, we have*

$$\left(\overline{x}_{k|k}^{i,a^i,1}, P_{k|k}^{i,a^i,1}, \ell_{k|k}^{i,a^i,1}\right) = \mathrm{u}_p\left(\overline{x}_{k|k-1}^{i,a^i,1}, P_{k|k-1}^{i,a^i,1}, z\right) \tag{44}$$

$$\begin{aligned} l_{k|k}^{i,a^i,Z_k^j} &= c_{k|k-1}^{i,a^i} p_1^D \ell_{k|k}^{i,a^i,1} \\ &\quad + \left(1 - c_{k|k-1}^{i,a^i}\right) p_2^D \ell_{k|k}^{i,a^i} \end{aligned} \tag{45}$$

$$c_{k|k}^{i,a^i} = \frac{c_{k|k-1}^{i,a^i} p_1^D \ell_{k|k}^{i,a^i,1}}{l_{k|k}^{i,a^i,Z_k^j}}. \tag{46}$$

For the new Bernoulli initiated by subset Z_k^j*, the single target density corresponding to an existing Bernoulli is*

$$\begin{aligned} f_{k|k}^{i,2}(x) &= c_{k|k}^{i,2} \sum_{q=1}^{n_{k|k-1}^p} w_1^q \mathcal{N}_p\left(x; \overline{x}_{k|k}^{i,2,q}, P_{k|k}^{i,2,q}\right) \\ &\quad + \left(1 - c_{k|k}^{i,2}\right) \sum_{q=1}^{n_{k|k-1}^e} w_2^q \mathcal{G}_e\left(x; \zeta_{k|k}^{i,2,q}\right) \end{aligned} \tag{47}$$

$$\left(\zeta_{k|k}^{i,2,q}, \ell_{2,k|k}^{i,2,q}\right) = \mathrm{u}_e\left(\zeta_{k|k-1}^{e,q}, Z_k^j\right) \tag{48}$$

$$w_{k|k}^{i,2} = \delta_1\left[\left|Z_k^j\right|\right] \left[\prod_{z \in Z_k^j} \lambda^C(z)\right] + l_{k|k}^{Z_k^j} \tag{49}$$

where $w_1^q \propto w_{k|k-1}^{p,q} \ell_{1,k|k}^{i,2,q}$ *and* $w_2^q \propto w_{k|k-1}^{e,q} \ell_{2,k|k}^{i,2,q}$*.*

For $m_k^j > 1$*,*

$$l_{k|k}^{Z_k^j} = p_2^D \sum_{q=1}^{n_{k|k-1}^e} w_{k|k-1}^{e,q} \ell_{2,k|k}^{i,2,q}, \tag{50}$$

$r_{k|k}^{i,2} = 1$ *and* $c_{k|k}^{i,2} = 0$*. For* $m_k^j = 1$*,* $Z_k^j = \{z\}$*, we have*

$$\left(\overline{x}_{k|k}^{i,2,q}, P_{k|k}^{i,2,q}, \ell_{1,k|k}^{i,2,q}\right) = \mathrm{u}_p\left(\overline{x}_{k|k-1}^{p,q,1}, P_{k|k-1}^{p,q,1}, z\right) \tag{51}$$

$$\begin{aligned} l_{k|k}^{Z_k^j} &= p_1^D \sum_{q=1}^{n_{k|k-1}^p} w_{k|k-1}^{p,q} \ell_{1,k|k}^{i,2,q} \\ &\quad + p_2^D \sum_{q=1}^{n_{k|k-1}^e} w_{k|k-1}^{e,q} \ell_{2,k|k}^{i,2,q} \end{aligned} \tag{52}$$

$$r_{k|k}^{i,2} = \frac{l_{k|k}^{Z_k^j}}{w_{k|k}^{i,a^i}} \tag{53}$$

$$c_{k|k}^{i,2} = \frac{p_1^D \sum_{q=1}^{n_{k|k-1}^p} w_{k|k-1}^{p,q} \ell_{1,k|k}^{i,2,q}}{l_{k|k}^{Z_k^j}}. \quad \square \tag{54}$$

Lemma 2 is obtained by using Theorem 1 and the GGIW and Gaussian updates [5], [19]. We can see that the number of components in the PPP corresponding to extended targets doubles in the update. This is due to the fact that the likelihood for misdetection for extended targets, see (24), has two terms $1 - p_2^D$ and $p_2^D e^{-\gamma}$. The first term corresponds to a misdetection obtained through the detection process modelled by p_2^D, whereas the second term corresponds to a misdetection obtained when the detection PPP generates zero measurements [5], [16], [32]. These terms create two updated PPP components for each prior PPP component. For the same reason, in the update of previous Bernoullis with a misdetection, the extended target updated density is a mixture of two GGIW, see (35). As only the Gamma distribution differs in the two updated GGIWs, we apply merging for Gamma densities [33] to obtain an updated single-target density of the form (28).

For the detection of previous Bernoullis, the hypothesis represents with probability $r_{k|k}^{i,a^i} = 1$ that there is target. If $m_k^j > 1$, the target is an extended target with probability one ($c_{k|k}^{i,a^i} = 0$). If $m_k^j = 1$, the target may be a point or an extended target. For the new Bernoulli components, if $m_k^j > 1$, the local hypotheses represent an existing extended target with probability one. For $m_k^j = 1$, the new Bernoulli may represent clutter, a single target or an extended target. All possible clutter events are accounted for in the hypotheses with $m_k^j = 1$ and so do not need to be duplicated in events with $m_k^j > 1$. We can also see that the single target density (47) for new Bernoulli components is a mixture for both point and extended targets. To obtain an updated density as in (28), we perform merging of the Gaussian mixtures and merging of the GGIW mixtures [33], [34].

It should be noted that, if the probability of detection is non-constant, it can be approximated as a constant at the predicted means for point and extended targets for each hypothesis [5, Tab. IV]. Then, we can perform the corresponding updates in Lemma 2.

C. Prediction

We consider that the probability of survival is a constant $p^S(\cdot) = p^S$ and linear/Gaussian dynamics for point targets. That is, for $x \in \mathbb{R}^{n_x}$, we have

$$g(\cdot \,|x) = \mathcal{N}(\cdot; Fx, Q) \tag{55}$$

where F is the transition matrix and Q is the process noise covariance matrix. For GGIW targets, there are several dynamic models [7], [8]. In the simulations, we use the one in [5]. We also assume that a point target cannot become an extended target and vice versa. The target birth intensity is of the form

$$\lambda_k^B(x) = \sum_{q=1}^{n_k^{b,p}} w_k^{b,p,q} \mathcal{N}_p\left(x; \overline{x}_k^{b,p,q,1}, P_k^{b,p,q,1}\right)$$

$$+\sum_{q=1}^{n_k^{b,e}} w_k^{b,e,q}\mathcal{G}_e\left(x;\zeta_k^{b,e,q}\right). \tag{56}$$

We apply the PMBM prediction step [11], [12] to obtain a PMBM with the following parameters. Given a single-target filtering density $f_{k-1|k-1}^{i,a^i}(\cdot)$ of the form (28), then the predicted density is of the same form with $c_{k|k-1}^{i,a^i}=c_{k-1|k-1}^{i,a^i}$ and

$$\zeta_{k|k-1}^{i,a^i}=\mathrm{p}_e\left(\zeta_{k-1|k-1}^{i,a^i}\right) \tag{57}$$

$$\left(\overline{x}_{k|k-1}^{i,a^i,1},P_{k|k-1}^{i,a^i,1}\right)=\mathrm{p}_p\left(\overline{x}_{k-1|k-1}^{i,a^i,1},P_{k-1|k-1}^{i,a^i,1}\right) \tag{58}$$

where $\mathrm{p}_p(\cdot)$ and $\mathrm{p}_e(\cdot)$ denote the Kalman filter [19] and the extended target GGIW prediction [5, Tab. III], respectively.

The predicted PPP is

$$\lambda_{k|k-1}(x)=\sum_{q=1}^{n_{k-1|k-1}^{p}} p^S w_{k-1|k-1}^{p,q}\mathcal{N}_p\left(x;\overline{x}_{k|k-1}^{p,q,1},P_{k|k-1}^{p,q,1}\right)+\sum_{q=1}^{n_{k-1|k-1}^{e}} p^S w_{k-1|k-1}^{e,q}\mathcal{G}_e\left(x;\zeta_{k|k-1}^{e,q}\right)+\lambda_k^B(x)$$

where $\left(\overline{x}_{k|k-1}^{p,q,1},P_{k|k-1}^{p,q,1}\right)=\mathrm{p}_p\left(\overline{x}_{k-1|k-1}^{p,q,1},P_{k-1|k-1}^{p,q,1}\right)$ and $\zeta_{k|k-1}^{e,q}=\mathrm{p}_e\left(\zeta_{k-1|k-1}^{e,q}\right)$.

While this prediction step assumes that there is no dynamic change between point and extended targets (e.g., the targets are pedestrians and vehicles), in some applications, a point target may become an extended target if it gets sufficiently close to the sensor. In this setting, one should design the corresponding transition density to capture this.

D. PMB approximation

It is also useful to consider a PMB approximation to the PMBM (1) to develop a faster algorithm. If we perform this approximation after each update, we obtain the corresponding PMB filter [11], [35]. Given an updated PMBM (1) with $k'=k$, the track-oriented PMB approximation is

$$f_{k|k}^{\mathrm{pmb}}(X_k)=\sum_{Y\uplus W=X_k} f_{k|k}^{\mathrm{p}}(Y)\,f_{k|k}^{\mathrm{mb}}(W) \tag{59}$$

$$f_{k|k}^{\mathrm{mb}}(X_k)=\sum_{\uplus_{l=1}^{n_{k|k}}X^l=X_k}\prod_{i=1}^{n_{k|k}} f_{k|k}^{i}\left(X^i\right) \tag{60}$$

where $f_{k|k}^{i}(\cdot)$ is a Bernoulli density with probability r^i of existence and single target density $p^i(\cdot)$ such that

$$r^i=\sum_{a^i=1}^{h^i}\overline{w}_{k|k}^{i,a^i}r_{k|k}^{i,a^i} \tag{61}$$

$$p^i(x)=\frac{\sum_{a^i=1}^{h^i}\overline{w}_{k|k}^{i,a^i}r_{k|k}^{i,a^i}f_{k|k}^{i,a^i}(x)}{r^i} \tag{62}$$

$$\overline{w}_{k|k}^{i,a^i}=\sum_{b\in\mathcal{A}_{k|k}:b^i=a^i} w_{k|k}^{b}. \tag{63}$$

The PMB approximation (59)-(60) minimises the Kullback-Leibler divergence (KLD) on a single target space augmented with an auxiliary variable, which represents if the target remains undetected or corresponds to the i-th Bernoulli component [36]. We can see that (62) is a mixture over all local hypotheses and that the PPP part of the PMBM (1) is not affected by the PMB approximation.

In the implementation for coexisting point-extended targets, we are interested in single target densities of the form (28). By using moment matching (KLD minimisation) for the mixture in $p^i(\cdot)$, we obtain the single-target density

$$p^i(x)=c^i\mathcal{N}_p\left(x;\overline{x}_{k|k}^{i},P_{k|k}^{i}\right)+\left(1-c^i\right)\mathcal{G}_e\left(x;\zeta_{k|k}^{i}\right) \tag{64}$$

$$c^i=\frac{\sum_{a^i=1}^{h^i}\overline{w}_{k|k}^{i,a^i}r_{k|k}^{i,a^i}c_{k|k}^{i,a^i}}{r^i} \tag{65}$$

$$\left(\overline{x}_{k|k}^{i},P_{k|k}^{i}\right)=\mathrm{m}_{\mathrm{G}}\left(\overline{x}_{k|k}^{i,a^1,1},P_{k|k}^{i,a^1,1},...,\overline{x}_{k|k}^{i,a^{h^i},1},P_{k|k}^{i,a^{h^i},1},\beta_{\mathrm{G}}^{i,a^1},...,\beta_{\mathrm{G}}^{i,a^{h^i}}\right) \tag{66}$$

$$\beta_{\mathrm{G}}^{i,a^i}\propto\overline{w}_{k|k}^{i,a^i}r_{k|k}^{i,a^i}c_{k|k}^{i,a^i} \tag{67}$$

$$\zeta_{k|k}^{i}=\mathrm{m}_{\mathrm{GG}}\left(\zeta_{k|k}^{i,a^1},...,\zeta_{k|k}^{i,a^{h^i}},\beta_{\mathrm{GG}}^{i,a^1},...,\beta_{\mathrm{GG}}^{i,a^{h^i}}\right) \tag{68}$$

$$\beta_{\mathrm{GG}}^{i,a^i}\propto\overline{w}_{k|k}^{i,a^i}r_{k|k}^{i,a^i}\left(1-c_{k|k}^{i,a^i}\right) \tag{69}$$

where $\mathrm{m}_{\mathrm{G}}(\cdot)$ is a function that obtains the mean and covariance of a Gaussian mixture with weights $\beta_{\mathrm{G}}^{i,a^1},...,\beta_{\mathrm{G}}^{i,a^{h^i}}$ (normalised to sum to one) and moments $\overline{x}_{k|k}^{i,a^1,1},P_{k|k}^{i,a^1,1},...,\overline{x}_{k|k}^{i,a^{h^i},1},P_{k|k}^{i,a^{h^i},1}$ [37]. The function $\mathrm{m}_{\mathrm{GG}}(\cdot)$ obtains the GGIW parameters that minimise the KLD from a mixture with weights $\beta_{\mathrm{GG}}^{i,a^1},...,\beta_{\mathrm{GG}}^{i,a^{h^i}}$ (normalised to sum to one) and parameters $\zeta_{k|k}^{i,a^1},...,\zeta_{k|k}^{i,a^{h^i}}$ [33], [34].

E. Target state estimation

Given a PMBM posterior, we can apply several estimators to estimate the current set of targets, see details in [12, Sec. VI]. We proceed to explain how Estimator 1 in [12, Sec. VI], which is the one we use in the simulations, is adapted to deal with the single-target space $\mathcal{X}=\mathbb{R}^{n_x}\uplus\mathcal{X}_e$.

We first obtain the global hypothesis with highest weight and select its Bernoulli components whose probability of existence is above a threshold (0.5 in the simulations). For each of these Bernoulli components, which have densities of the form (28), we estimate a target state, which may be a point or an extended target. If the probability of being a point target is $c_{k|k}^{i,a^i}>0.5$, then we estimate a point target located at the mean $\overline{x}_{k|k}^{i,a^i,1}$. Otherwise, we estimate an extended target with kinematic and extent states located at the mean [8]

$$\hat{\xi}_k=\overline{x}_{k|k}^{i,a^i,2} \tag{70}$$

$$\hat{X}_k=\frac{V_{k|k}^{i,a^i}}{v_{k|k}^{i,a^i}-2d-2}. \tag{71}$$

F. Practical aspects

As in other multiple target filters with data associations, the number of global and local hypotheses increases unboundedly in time. Therefore, in practice, it is necessary to perform approximations, with the objective of only propagating hypotheses with relevant weights. In fact, due to the structure of the hypotheses of Theorem 1, the way to handle the data association problem with coexisting point and extended targets is quite similar to the extended target case [5], [7].

In our implementation, the PMBM posterior is represented by a list of Bernoullis $i \in \{1, ..., n_{k|k'}\}$, where each of them contains their local hypotheses with their parameters, a global hypothesis table, which contains indices to local hypotheses of each Bernoulli, and a vector with the global hypotheses weights. To deal with the data association problem at each update, we first perform gating to obtain two sets of measurements: 1) measurements that are in the gate of at least one previous Bernoulli, and 2) measurements that are only in the gate of the PPP components. Measurements that do not fall into these categories are discarded.

For the set of measurements in group 1), we first generate possible partitions of this set using the DBSCAN algorithm with distance thresholds between $\Gamma_{d,min}$ and $\Gamma_{d,max}$, with a step size of ε_d [38], [39]. The minimum number of points to form a region, which is a parameter of the DBSCAN algorithm, is set to 1 to capture point-target measurements. Among the possible partitions generated by the multiple runs of DBSCAN algorithms, there may be repeated ones, so we keep the unique ones and we obtain the unique subsets of measurements in these partitions. These subsets are then used to generate the updated local hypotheses for previous Bernoullis, see (8)-(16). A new Bernoulli component is also created for each unique subset of measurements that is in the gate of a GGIW PPP component. For each previous global hypothesis and partition, obtained by DBSCAN, we run Murty's algorithm [40] to find the global hypotheses with highest weights.

For the set of measurements in group 2), which may correspond to newly detected targets, we run the DBSCAN to obtain possible partitions. Each of these partitions in theory gives rise to different global hypotheses corresponding to new born targets. We simplify this procedure by finding the partition with highest weight and only generating the Bernoulli components that are generated by the sets in this partition [5]. These new Bernoulli components are added to all the global hypotheses, whose weights remain unchanged.

We would like to point out that, while DBSCAN is a fast method for clustering, it is agnostic to target shape. Therefore, in difficult scenarios, it may be suitable to consider further partitions using additional methods that account for target shape, for example, prediction partition and expectation maximisation partition [32], [41].

We also perform pruning of global hypotheses with low weights, and pruning of Bernoulli components with low existence probabilities [12], [13], [42]. A pseudocode of the resulting PMBM update is provided in Algorithm 1. The PMB filter performs the same PMBM update and it is then followed by the PMB approximation, see Section IV-D. It is also possible to approximate the PMB marginal data association probabilities directly using belief propagation [43]–[45].

Algorithm 1 Pseudocode of the PMBM update

- Perform gating to separate current measurements into the following disjoint categories:
  - ○ 1. A set of measurements that are in the gate of at least one previous Bernoulli.
  - ○ 2. A set of measurements that are only in the gate of PPP components.
- For measurements corresponding to 1:
  - ○ Run DBSCAN to generate possible partitions.
  - ○ Obtain unique subsets in the previous partitions.
  - ○ Generate new local hypotheses for previous Bernoullis.
  - ○ Generate new Bernoulli components.
  - ○ For each previous global hypothesis, run Murty's algorithm to obtain updated global hypotheses.
- Perform pruning of global hypotheses and Bernoulli components.
- For measurements corresponding to 2 (new targets):
  - ○ Run DBSCAN to generate possible partitions.
  - ○ Find the partition with highest weight.
  - ○ Generate the new Bernoulli components for this partition.
  - ○ Add these Bernoullis to the global hypotheses.

V. Simulations

In this section, we assess the PMBM and PMB filters for coexisting point and extended targets via numerical simulations[2]. In this section, we refer to these filters as point-extended PMBM and PMB (PE-PMBM and PE-PMB) filters. The filters are implemented with the following parameters: maximum number of hypotheses 20, threshold for pruning the PPP weights 10^{-5}, threshold for pruning Bernoulli components 10^{-3} and threshold for pruning global hypotheses 10^{-3}. The DBSCAN algorithm [38] is run with distance thresholds between $\Gamma_{d,min} = 0.1$ and $\Gamma_{d,max} = 12$, with a step size of $\varepsilon_d = 0.1$. We have also implemented a point-extended MBM (PE-MBM) filter, see Section III-C.

Extended target filters can in principle deal with point-target detections, as they do not place zero probability to this event. Therefore, we compare the proposed filters with extended target PMBM and PMB filters, which we refer to as E-PMBM and E-PMB filters [5], [39]. We proceed to discuss the models and the simulations results. All the units in this section are given in the international system.

A. Models

We consider a point target state $[p_x, \dot{p}_x, p_y, \dot{p}_y]^T$, which contains position and velocity in a two-dimensional plane. Point targets move with a nearly-constant velocity model with

$$F = I_2 \otimes \begin{pmatrix} 1 & \tau \\ 0 & 1 \end{pmatrix}, \quad Q = qI_2 \otimes \begin{pmatrix} \tau^3/3 & \tau^2/2 \\ \tau^2/2 & \tau \end{pmatrix}$$

where $\tau = 1$, $q = 0.25$, $\otimes$ denotes Kronecker product and I_2 is an identity matrix of size 2. The probability of survival is $p^S = 0.99$. The extended target model is the GGIW model in Section IV. Extended targets move with the previous nearly-constant

[2]Matlab code is available at https://github.com/Agarciafernandez and https://github.com/yuhsuansia.

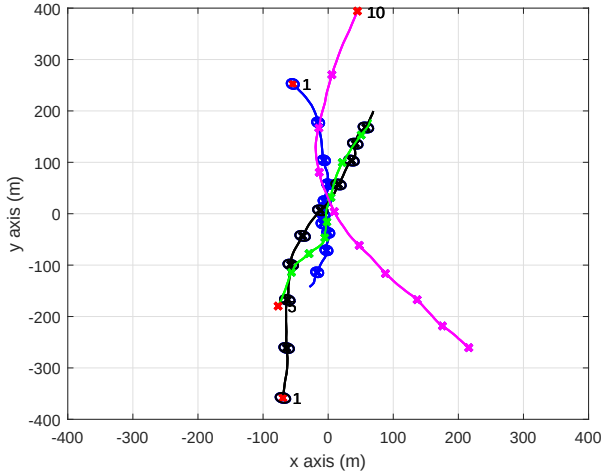

Fig. 1: Scenario of the simulations. Two extended targets are born at time step 1 and two point targets are born at time steps 5 and 10. The extended targets are alive at all time steps. The last time steps of the point targets are 38 and 60. Targets are in close proximity at around time step 50. Target states at time of birth are marked with a red cross, and every 10 time steps with a cross. The 3-σ ellipse for extended targets is shown every 10 time steps.

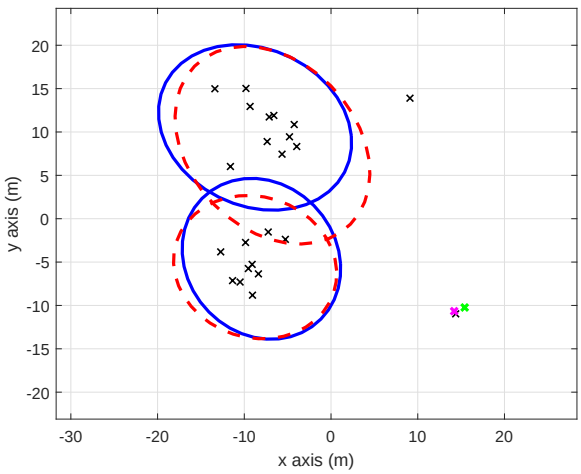

Fig. 2: Ground truth and estimated set of targets at time step 52 in an illustrative run. Measurements are shown as black crosses. Blue ellipses represent the true extended targets, a green cross represents the true point target. The red, dashed ellipses represent the estimated extended targets and the pink cross represents the estimated point target. The three targets are properly detected and classified. At this time step, there are 22 measurements within the gate of the previous targets (the three targets shown in the figure). The output of the DBSCAN algorithm with different distance thresholds produces 18 partitions of these measurements, ranging from partitions with 22 clusters (each with a single measurement) to 2 clusters.

velocity model and their extent matrix and γ parameter remain constant. The probability of survival is 0.99.

The birth model is a PPP of the form (56). The PPP point target part has parameters $n_k^{b,p} = 1$, $w_k^{b,p,1} = 0.03$, $\overline{x}_k^{b,p,1,1} = [0,0,0,0]^T$, $P_k^{b,p,1,1} = \mathrm{diag}([200^2, 4^2, 200^2, 4^2])$. The extended target part has: $n_k^{b,e} = 1$, $w_k^{b,e,1} = 0.06$, and

$$\zeta_k^{b,e,q} = \left(40, 4, \overline{x}_k^{b,p,1,1}, P_k^{b,p,1,1}, 20, 200 I_2\right).$$

As the birth covariance matrix is large, new born targets may appear in a large area. The multi-Bernoulli birth model for the PE-MBM filter has a single Bernoulli with existence probability 0.06, point-target probability $c = 1/3$, point target mean $\overline{x}_k^{b,p,1,1}$ and covariance $P_k^{b,p,1,1}$, and GGIW $\zeta_k^{b,e,q}$.

We measure the positions of the targets. For point targets, we have parameters: $p_1^D = 0.95$, and

$$H_1 = \begin{pmatrix} 1 & 0 & 0 & 0 \\ 0 & 0 & 1 & 0 \end{pmatrix}, \quad R = \sigma^2 I_2$$

where $\sigma^2 = 1$. For extended targets, the parameters are $p_2^D = p_1^D$, $H_2 = H_1$. Clutter is uniformly distributed in the surveillance area $[-500, 500] \times [-500, 500]$ with an average of $\lambda^C = 8$ false alarms per scan. We consider 100 time steps and the set of trajectories shown in Figure 1, which has been obtained by sampling from the dynamic process. The E-PMBM and E-PMB filters are recovered by setting the birth intensity for point targets to zero in the PE-PMBM and PE-PMB filters.

B. Results

We first show the ground truth and the estimate of the set of targets at time step 52 in an illustrative run with the PE-PMBM filter in Figure 2. We can see that the each extended target generates several measurements and are detected. The ellipses of the estimated targets are reasonably accurate. The point target generates a single measurement at this time step, and it is also detected. Its estimate is close to its true state. In this scenario, the class probability quickly reaches either zero or one for the considered targets, classifying all targets correctly.

We evaluate filter performance via Monte Carlo simulation with 100 runs. We compute the error between the true set of targets at each time and its estimate using the generalised optimal subpattern assignment (GOSPA) metric with parameters $\alpha = 2$, $p = 2$, $c = 10$, and its decomposition into localisation errors and costs for missed and false targets [46]. The base metric for target states is the Gaussian Wasserstein distance, which measures error for position and extent [47]. In the base metric, we consider a point target as an extended target with extent zero.

The root mean square GOSPA (RMS-GOSPA) error against time and its decomposition are shown in Figure 3. We can see that PE-PMBM and PE-PMB filter perform quite similarly and outperform E-PMBM and E-PMB. PE-MBM performs quite similarly to PE-PMBM and PE-PMB but does not detect one of the targets at time step 1, as the birth model sets the maximum number of new born targets to one. For PE-PMBM and PE-PMB, missed target errors are higher when new targets are born. False target errors are higher when targets die and when targets get in close proximity. Localisation errors are higher at the beginning of the simulation, and when targets get in close proximity, as the data association problem is more complicated. ET-PMBM and ET-PMB also behave quite similarly and have more difficulty in detecting the point targets, so they show a higher missed target error at some time

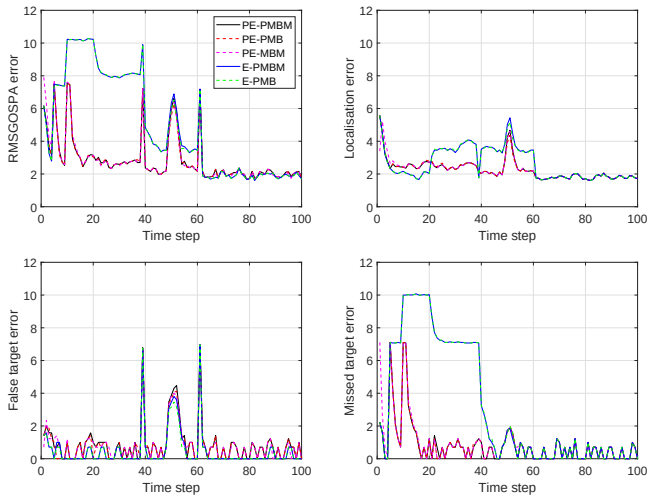

Fig. 3: RMS-GOSPA error (m) for the position elements and its decomposition. The PE-PMBM and PE-PMB filters have very similar performance. PE-MBM fails to detect one of the targets at time step 1. The E-PMBM and E-PMB have a higher error at some time steps due to missed point targets. E-PMBM and E-PMB localisation errors are also higher at some time steps, as point targets are estimated with some extent.

steps. In addition, the localisation error is also higher at some time steps, as point targets are estimated with a certain extent, which increases the error compared to the ground truth.

The running times of the Matlab implementations (100 time steps) on an Intel Core i5 laptop are: 56.4s (PE-PMBM), 17.5s (PE-PMB), 64.5 (PE-MBM), 25.5s (E-PMBM) and 15.2 (E-PMB). The PMB filters are considerably faster than PMBM/MBM, as they do not propagate a mixture through the filtering recursion. Only considering extended targets is also faster, though it decreases performance.

To provide more complete simulation results, we show the RMS-GOSPA errors, along with the GOSPA error decomposition, considering all time steps for different values of the probability of detection and clutter rate in Table I. Due to space constraints, we do not show E-PMB, which behaves quite similarly to E-PMBM. In this table, "Tot.", "Loc.", "Fal." and "Mis." refer to total GOSPA, localisation, false target and missed target costs, respectively. The filters with coexisting point extended targets consistently provide more accurate results, especially due to a lower number of missed targets. The PE-PMBM and PE-PMB filters provide quite similar results though the PE-PMB filter is slightly better. While the PE-PMBM filter provides the closed-form solution to the filtering recursion, we apply approximations and an suboptimal estimator, so the PE-PMB filter may work better in some scenarios. Decreasing the probability of detection or increasing the clutter rate, the GOSPA error for all filters increases, mainly due to a rise in missed target cost.

VI. Conclusions

We have derived the update of a PMBM filter with a measurement model that can consider point and extended targets, and we have shown that the updated posterior is also a PMBM. We have also proposed an implementation of the resulting PMBM recursion to consider coexisting point and extended targets. In order to do so, we first set the suitable single-target space and single target densities, which are based on Gaussian densities for single targets, and GGIW densities for extended targets. Finally, based on the previous results, we have explained how to obtain a computationally-lighter PMB filter for coexisting point and extended targets.

We think there are many lines of future work. In many applications, there are coexisting point and extended targets, and one can perform research into tailored measurement and target models for each application. Another line of future work is to extend the above results to consider PMBMs on sets of trajectories, with coexisting point and extended targets, to provide full trajectory information [21], [27], [28].

References

[1] J. Choi, S. Ulbrich, B. Lichte, and M. Maurer, "Multi-target tracking using a 3D-lidar sensor for autonomous vehicles," in *16th International IEEE Conference on Intelligent Transportation Systems*, 2013, pp. 881–886.

[2] E. F. Brekke *et al.*, "The Autosea project: Developing closed-loop target tracking and collision avoidance systems," *Journal of Physics: Conference Series*, vol. 1357, pp. 1–12, Oct. 2019.

[3] R. P. S. Mahler, *Advances in Statistical Multisource-Multitarget Information Fusion*. Artech House, 2014.

[4] A. Saucan, M. J. Coates, and M. Rabbat, "A multisensor multi-Bernoulli filter," *IEEE Transactions on Signal Processing*, vol. 65, no. 20, pp. 5495–5509, 2017.

[5] K. Granström, M. Fatemi, and L. Svensson, "Poisson multi-Bernoulli mixture conjugate prior for multiple extended target filtering," *IEEE Transactions on Aerospace and Electronic Systems*, vol. 56, no. 1, pp. 208–225, Feb. 2020.

[6] S. S. Blackman, "Multiple hypothesis tracking for multiple target tracking," *IEEE Aerospace and Electronic Systems Magazine*, vol. 19, no. 1, pp. 5–18, Jan. 2004.

[7] K. Granström, M. Baum, and S. Reuter, "Extended object tracking:introduction, overview, and applications," *Journal of Advances in Information Fusion*, vol. 12, no. 2, pp. 139–174, Dec. 2017.

[8] J. W. Koch, "Bayesian approach to extended object and cluster tracking using random matrices," *IEEE Transactions on Aerospace and Electronic Systems*, vol. 44, no. 3, pp. 1042–1059, Jul. 2008.

[9] K. Gilholm, S. Godsill, S. Maskell, and D. Salmond, "Poisson models for extended and group tracking," in *Proc. SPIE 5913, Signal and Data Processing of Small Targets*, vol. 5913, 2005, pp. 1–12.

[10] X. Tang, M. Li, R. Tharmarasa, and T. Kirubarajan, "Seamless tracking of apparent point and extended targets using Gaussian process PMHT," *IEEE Transactions on Signal Processing*, vol. 67, no. 18, pp. 4825–4838, Sep. 2019.

[11] J. L. Williams, "Marginal multi-Bernoulli filters: RFS derivation of MHT, JIPDA and association-based MeMBer," *IEEE Transactions on Aerospace and Electronic Systems*, vol. 51, no. 3, pp. 1664–1687, July 2015.

[12] A. F. García-Fernández, J. L. Williams, K. Granström, and L. Svensson, "Poisson multi-Bernoulli mixture filter: direct derivation and implementation," *IEEE Transactions on Aerospace and Electronic Systems*, vol. 54, no. 4, pp. 1883–1901, Aug. 2018.

[13] A. F. García-Fernández, Y. Xia, K. Granström, L. Svensson, and J. L. Williams, "Gaussian implementation of the multi-Bernoulli mixture filter," in *Proceedings of the 22nd International Conference on Information Fusion*, 2019.

[14] B. T. Vo and B. N. Vo, "Labeled random finite sets and multi-object conjugate priors," *IEEE Transactions on Signal Processing*, vol. 61, no. 13, pp. 3460–3475, July 2013.

[15] M. Beard, S. Reuter, K. Granström, B. Vo, B. Vo, and A. Scheel, "Multiple extended target tracking with labeled random finite sets," *IEEE Transactions on Signal Processing*, vol. 64, no. 7, pp. 1638–1653, 2016.

[16] C. Lundquist, K. Granström, and U. Orguner, "An extended target CPHD filter and a gamma Gaussian inverse Wishart implementation," *IEEE Journal of Selected Topics in Signal Processing*, vol. 7, no. 3, pp. 472–483, June 2013.

TABLE I: RMS-GOSPA errors and their decompositions for the filters and different parameters

		PE-PMBM				PE-PMB				PE-MBM				E-PMBM			
$p_1^D = p_2^D$	λ_c	Tot.	Loc.	Fal.	Mis.	Tot.	Loc.	Fal.	Mis.	Tot.	Loc.	Fal.	Mis.	Tot.	Loc.	Fal.	Mis.
0.95	8	3.21	2.36	1.50	1.57	3.18	2.35	1.46	1.56	3.27	2.36	1.45	1.73	5.81	2.83	1.29	4.91
0.95	16	3.38	2.48	1.54	1.70	3.35	2.46	1.51	1.70	3.49	2.45	1.42	2.04	6.91	2.14	0.86	6.52
0.85	8	3.70	2.61	1.90	1.81	3.65	2.60	1.80	1.82	3.84	2.52	1.42	2.54	6.54	2.74	1.31	5.79
0.85	16	3.78	2.60	1.86	2.02	3.77	2.64	1.80	2.01	4.09	2.51	1.33	2.94	7.10	2.25	0.88	6.68

[17] Y. Ge, F. Wen, H. Kim, M. Zhu, S. Kim, L. Svensson, and H. Wymeersch, "5G SLAM using the clustering and assignment approach with diffuse multipath," *Sensors*, vol. 20, 4656.

[18] T. Kurien, "Issues in the design of practical multitarget tracking algorithms," in *Multitarget-Multisensor Tracking: Advanced Applications*, Y. Bar-Shalom, Ed. Artech House, 1990.

[19] S. Särkkä, *Bayesian Filtering and Smoothing*. Cambridge University Press, 2013.

[20] K. Granström, A. Natale, P. Braca, G. Ludeno, and F. Serafino, "Gamma Gaussian inverse Wishart probability hypothesis density for extended target tracking using X-band marine radar data," *IEEE Transactions on Geoscience and Remote Sensing*, vol. 53, no. 12, pp. 6617–6631, Dec. 2015.

[21] Y. Xia, K. Granström, L. Svensson, A. F. García-Fernández, and J. L. Williams, "Extended target Poisson multi-Bernoulli mixture trackers based on sets of trajectories," in *Proceedings of the 22nd International Conference on Information Fusion*, 2019.

[22] T. J. Broida, S. Chandrashekhar, and R. Chellappa, "Recursive 3-D motion estimation from a monocular image sequence," *IEEE Transactions on Aerospace and Electronic Systems*, vol. 26, no. 4, pp. 639–656, Jul. 1990.

[23] L. Hammarstrand, L. Svensson, F. Sandblom, and J. Sorstedt, "Extended object tracking using a radar resolution model," *IEEE Transactions on Aerospace and Electronic Systems*, vol. 48, no. 3, pp. 2371–2386, Jul. 2012.

[24] B. Ristic and J. Sherrah, "Bernoulli filter for joint detection and tracking of an extended object in clutter," *IET Radar, Sonar Navigation*, vol. 7, no. 1, pp. 26–35, Jan. 2013.

[25] X. Shen, Z. Song, H. Fan, and Q. Fu, "General Bernoulli filter for arbitrary clutter and target measurement processes," *IEEE Signal Processing Letters*, vol. 25, no. 10, pp. 1525–1529, Oct. 2018.

[26] R. Mahler, B.-T. Vo, and B.-N. Vo, "CPHD filtering with unknown clutter rate and detection profile," *IEEE Transactions on Signal Processing*, vol. 59, no. 8, pp. 3497–3513, Aug. 2011.

[27] A. F. García-Fernández, L. Svensson, and M. R. Morelande, "Multiple target tracking based on sets of trajectories," *IEEE Transactions on Aerospace and Electronic Systems*, vol. 56, no. 3, pp. 1685–1707, Jun. 2020.

[28] Y. Xia, K. Granström, L. Svensson, A. F. García-Fernández, and J. L. Wlliams, "Multi-scan implementation of the trajectory Poisson multi-Bernoulli mixture filter," *Journal of Advances in Information Fusion*, vol. 14, no. 2, pp. 213–235, Dec. 2019.

[29] E. Mazor, A. Averbuch, Y. Bar-Shalom, and J. Dayan, "Interacting multiple model methods in target tracking: a survey," *IEEE Transactions on Aerospace and Electronic Systems*, vol. 34, no. 1, pp. 103–123, Jan. 1998.

[30] M. Feldmann, D. Fränken, and W. Koch, "Tracking of extended objects and group targets using random matrices," *IEEE Transactions on Signal Processing*, vol. 59, no. 4, pp. 1409–1420, Apr. 2011.

[31] A. K. Gupta and D. K. Nagar, *Matrix Variate Distributions*. Chapman & Hall, 1999.

[32] K. Granström and U. Orguner, "A PHD filter for tracking multiple extended targets using random matrices," *IEEE Transactions on Signal Processing*, vol. 60, no. 11, pp. 5657–5671, Nov. 2012.

[33] K. Granström and U. Orguner, "Estimation and maintenance of measurement rates for multiple extended target tracking," in *15th International Conference on Information Fusion*, 2012, pp. 2170–2176.

[34] ——, "On the reduction of Gaussian inverse Wishart mixtures," in *15th International Conference on Information Fusion*, 2012, pp. 2162–2169.

[35] J. L. Williams, "An efficient, variational approximation of the best fitting multi-Bernoulli filter," *IEEE Transactions on Signal Processing*, vol. 63, no. 1, pp. 258–273, Jan. 2015.

[36] A. F. García-Fernández, L. Svensson, J. L. Williams, Y. Xia, and K. Granström, "Trajectory Poisson multi-Bernoulli filters," *IEEE Transactions on Signal Processing*, vol. 68, pp. 4933–4945, 2020.

[37] C. M. Bishop, *Pattern Recognition and Machine Learning*. Springer, 2006.

[38] M. Ester, H.-P. Kriegel, J. Sander, and X. Xu, "A density-based algorithm for discovering clusters in large spatial datasets with noise," in *2nd International Conference on Knowledge Discovery and Data Mining*, 1996, pp. 226–231.

[39] Y. Xia, K. Granström, L. Svensson, M. Fatemi, A. F. García-Fernández, and J. L. Williams, "Poisson multi-Bernoulli approximations for multiple extended object filtering," 2021. [Online]. Available: https://arxiv.org/abs/1801.01353

[40] K. G. Murty, "An algorithm for ranking all the assignments in order of increasing cost." *Operations Research*, vol. 16, no. 3, pp. 682–687, 1968.

[41] K. Granström, L. Svensson, S. Reuter, Y. Xia, and M. Fatemi, "Likelihood-based data association for extended object tracking using sampling methods," *IEEE Transactions on Intelligent Vehicles*, vol. 3, no. 1, pp. 30–45, March 2018.

[42] A. F. García-Fernández and S. Maskell, "Continuous-discrete multiple target filtering: PMBM, PHD and CPHD filter implementations," *IEEE Transactions on Signal Processing*, vol. 68, pp. 1300–1314, 2020.

[43] F. Meyer and J. L. Williams, "Scalable detection and tracking of extended objects," in *IEEE International Conference on Acoustics, Speech and Signal Processing*, 2020, pp. 8916–8920.

[44] F. Meyer and M. Z. Win, "Scalable data association for extended object tracking," *IEEE Transactions on Signal and Information Processing over Networks*, vol. 6, pp. 491–507, 2020.

[45] F. Meyer, T. Kropfreiter, J. L. Williams, R. Lau, F. Hlawatsch, P. Braca, and M. Z. Win, "Message passing algorithms for scalable multitarget tracking," *Proceedings of the IEEE*, vol. 106, no. 2, pp. 221–259, Feb. 2018.

[46] A. S. Rahmathullah, A. F. García-Fernández, and L. Svensson, "Generalized optimal sub-pattern assignment metric," in *20th International Conference on Information Fusion*, 2017, pp. 1–8.

[47] S. Yang, M. Baum, and K. Granström, "Metrics for performance evaluation of elliptic extended object tracking methods," in *IEEE International Conference on Multisensor Fusion and Integration for Intelligent Systems*, 2016, pp. 523–528.

Supplementary material: A Poisson multi-Bernoulli mixture filter for co-existing point and extended targets

APPENDIX A

In this appendix, we prove Theorem 1, which provides the update step, making use of probability generating functionals (PGFLs). A PGFL is an alternative representation of a multi-object density, in the same way as Fourier and z-transforms are for signals defined in the time domain.

For a multi-object density $f(\cdot)$, its PGFL $G_f[\cdot]$ is given by the set integral [3]

$$G_f[h] = \int h^X f(X)\delta X \tag{72}$$

where $h(\cdot)$ is a unitless function of state space, and $h^X = \prod_{x\in X} h(x)$, $h^{\emptyset} = 1$. The test function for PGFLs related to densities defined for targets and measurements are denoted as $h(\cdot)$ and $g(\cdot)$, respectively.

Given the PGFL $G_f[\cdot]$, we can recover its multi-object density $f(\cdot)$ by the set derivative [3]

$$f(X) = \frac{\delta}{\delta X} G_f[h]\bigg|_{h=0}. \tag{73}$$

A. PGFLs of targets and measurements

The density (1) in PGFL form is represented as [11]

$$G_{k|k'}[h] = G^{\mathrm{p}}_{k|k'}[h] \cdot G^{\mathrm{mbm}}_{k|k'}[h] \tag{74}$$

$$G^{\mathrm{p}}_{k|k'}[h] = \exp\left(\langle \lambda_{k|k'}, h-1\rangle\right) \propto \exp\left(\langle \lambda_{k|k'}, h\rangle\right) \tag{75}$$

$$G^{\mathrm{mbm}}_{k|k'}[h] = \sum_{a\in\mathcal{A}_{k'|k}} w^a_{k|k'} \prod_{i=1}^{n_{k'|k}} G^{i,a^i}_{k|k'}[h] \tag{76}$$

$$\propto \sum_{a\in\mathcal{A}_{k'|k}} \prod_{i=1}^{n_{k|k'}} \left[w^{i,a^i}_{k|k'} G^{i,a^i}_{k|k'}[h]\right] \tag{77}$$

where

$$G^{i,a^i}_{k|k'}[h] = 1 - r^{i,a^i}_{k|k'} + r^{i,a^i}_{k|k'} \langle f^{i,a^i}_{k|k'}, h\rangle. \tag{78}$$

Given the multi-target state X, measurements from each target are independent, and there is also independent PPP clutter. Therefore, the PGFL $G_Z[g|X]$ of the measurements given X is the product of PGFL

$$G_Z[g|X] = \exp\left(\langle \lambda^C, g-1\rangle\right) \prod_{x\in X} G[g|x] \tag{79}$$

where $G[g|x]$ is the PGFL of $f(Z|x)$.

B. Joint PGFL of targets and measurements

The joint PGFL of measurements and targets is [3], [11]

$$F[g,h] = \int\int g^{Z_k} h^{X_k} f(Z_k|X_k)\, f_{k|k-1}(X_k)\, \delta Z_k \delta X_k \tag{80}$$

$$= \int G[g|X_k] h^{X_k} f_{k|k-1}(X_k)\, \delta X_k \tag{81}$$

$$= \exp\left(\langle \lambda^C, g-1\rangle\right) G_{k|k-1}[hG_Z[g|\cdot]] \tag{82}$$

$$\propto \exp\left(\langle \lambda^C, g\rangle + \langle \lambda_{k|k-1}, hG[g|\cdot]\rangle\right) \times \sum_{a\in\mathcal{A}_{k|k-1}} \prod_{i=1}^{n_{k|k-1}} \left[w^{i,a^i}_{k|k-1} G^{i,a^i}_{k|k-1}\left[hG[g|\cdot]\right]\right]. \tag{83}$$

We denote the first line of (83) as

$$F^0[g,h] = \exp\left(\langle \lambda^C, g\rangle + \left\langle \lambda_{k|k-1}, hG[g|\cdot]\right\rangle\right) \tag{84}$$

which represents the joint PGFL of measurements (including false alarms) and targets in the PPP, up to a proportionality constant. We also denote

$$F^{i,a^i}[g,h] = G^{i,a^i}_{k|k-1}\left[hG[g|\cdot]\right] \tag{85}$$

$$= 1 - r^{i,a^i}_{k|k-1} + r^{i,a^i}_{k|k-1} \left\langle f^{i,a^i}_{k|k-1}, hG[g|\cdot]\right\rangle \tag{86}$$

which represents the joint PGFL of measurements (not including false alarms) and the i-th potential target. Then, using (5), we can write (83) as

$$F[g,h] \propto F^0[g,h] \sum_{a\in\mathcal{A}_{k|k-1}} \prod_{i=1}^{n_{k|k-1}} \left[w^{i,a}_{k|k-1} F^{i,a^i}[g,h]\right]. \tag{87}$$

C. Updated PGFL

We calculate the updated density $f_{k|k}(\cdot)$ via its PGFL $G_{k|k}[h]$, which is given by the set derivative of $F[g,h]$ w.r.t. Z_k evaluated at $g=0$ [3, Sec. 5.8] [11, Eq. (25)]

$$G_{k|k}[h] \propto \frac{\delta}{\delta Z_k} F[g,h]\bigg|_{g=0}. \tag{88}$$

Applying the product rule [11, Eq. (31)], we obtain

$$G_{k|k}[h] \propto \sum_{W_0 \uplus \cdots \uplus W_{n_{k|k-1}} = Z_k} \frac{\delta}{\delta W_0} F^0[g,h] \times \sum_{a\in\mathcal{A}_{k|k-1}} \prod_{i=1}^{n_{k|k-1}} \frac{\delta}{\delta W_i}\left(w^{i,a^i}_{k|k-1} F^{i,a^i}[g,h]\right)\bigg|_{g=0}. \tag{89}$$

The sum in (89) is over all decompositions of the measurement set Z into $(n_{k|k-1}+1)$ subsets, where one subset, W_0, represents measurements which are either false alarms, or correspond to a target represented by the PPP component (i.e., a target which has never been detected so far), and subset W_i, $i>0$, represents measurements assigned to the i-th Bernoulli.

We develop the required set derivatives over the following lemmas, starting with the Bernoulli component $F^i[g,h]$ in Section A-C1, and then moving on to the update of the PPP, $F^0[g,h]$, in Section A-C2.

1) Bernoulli update: We calculate the set derivative of $F^{i,a^i}[g,h]$. For $W_i \neq \emptyset$, we have

$$\frac{\delta}{\delta W_i} F^{i,a^i}[g,h] = r^{i,a^i}_{k|k-1} \left\langle f^{i,a^i}_{k|k-1}, h\frac{\delta}{\delta W_i} G[g|\cdot]\right\rangle \tag{90}$$

$$\frac{\delta}{\delta W_i} F^{i,a^i}[g,h]\bigg|_{g=0} = r^{i,a^i}_{k|k-1} \left\langle f^{i,a^i}_{k|k-1}, hf(W_i|\cdot)\right\rangle \tag{91}$$

where we have applied (73). For $W_i = \emptyset$, the set derivative does not change $F^{i,a^i}[g,h]$.

Equation (91) and $F^{i,a^i}[0,h]$ are the PGFL of a weighted Bernoulli component [11, Lem. 2] with parameters given in the following lemma.

Lemma 3. *The update of the weighted PGFL component $w^{i,a^i}_{k|k-1}G^{i,a^i}_{k|k-1}[h]$ (weighted Bernoulli) with measurement set W_i, i.e.,*

$$w^{i,a^i,W_i}_{k|k}G^{i,a^i,W_i}_{k|k}[h] = \frac{\delta}{\delta W_i}\left(w^{i,a^i}_{k|k-1}F^{i,a^i}[g,h]\right)\big|_{g=0}$$

is the PGFL of a weighted Bernoulli distribution, i.e., a distribution of the form [11, Lem. 2]

$$f^{i,a^i,W_i}_{k|k}(X) = w^{i,a^i,W_i}_{k|k} \times \begin{cases} 1 - r^{i,a^i,W_i}_{k|k} & X = \emptyset \\ r^{i,a^i,W_i}_{k|k} f^{i,a^i,W_i}_{k|k}(x) & X = \{x\} \\ 0 & |X| > 1 \end{cases} \tag{92}$$

where for $W_i = \emptyset$,

$$w^{i,a^i,W_i}_{k|k} = w^{i,a^i}_{k|k-1}\left[1 - r^{i,a^i}_{k|k-1} + r^{i,a^i}_{k|k-1}l^{i,a^i,W_i}_{k|k}\right] \tag{93}$$

$$l^{i,a^i,W_i}_{k|k} = \left\langle f^{i,a^i}_{k|k-1}, f(\emptyset|\cdot)\right\rangle \tag{94}$$

$$r^{i,a^i,W_i}_{k|k} = \frac{r^{i,a^i}_{k|k-1}l^{i,a^i,W_i}_{k|k}}{1 - r^{i,a^i}_{k|k-1} + r^{i,a^i}_{k|k-1}l^{i,a^i,W_i}_{k|k}} \tag{95}$$

$$f^{i,a^i,W_i}_{k|k}(x) = \frac{f^{i,a^i}_{k|k-1}(x)f(\emptyset|x)}{l^{i,a^i,W_i}_{k|k}}. \tag{96}$$

For $|W_i| \geq 1$,

$$w^{i,a^i,W_i}_{k|k} = w^{i,a^i}_{k|k-1}r^{i,a^i}_{k|k-1}l^{i,a^i,W_i}_{k|k} \tag{97}$$

$$l^{i,a^i,W_i}_{k|k} = \left\langle f^{i,a^i}_{k|k-1}, f(W_i|\cdot)\right\rangle \tag{98}$$

$$r^{i,a^i,W_i}_{k|k} = 1 \tag{99}$$

$$f^{i,a^i,W_i}_{k|k}(x) = \frac{f^{i,a^i}_{k|k-1}(x)\, f(W_i|x)}{l^{i,a^i,W_i}_{k|k}}. \tag{100}$$

This lemma therefore proves how to update a previous Bernoulli with a misdetection or a detection hypothesis in Theorem 1.

2) PPP update: We now turn to calculating the update of the PPP in (89) via the set derivative of $F^0[g,h]$, see (84).

Lemma 4. *The set derivative of $F^0[g,h]$ is*

$$\frac{\delta}{\delta W_0}F^0[g,h] = F^0[g,h]\sum_{P\angle W_0}\prod_{V\in P}d_V[g,h] \tag{101}$$

where

$$d_V[g,h] = \frac{\delta}{\delta V}\left(\langle\lambda^C, g\rangle + \left\langle\lambda_{k|k-1}, hG[g|\cdot]\right\rangle\right) \tag{102}$$

and $\sum_{P\angle W_0}$ denotes the sum over all partitions P of W_0. □

The proof of Lemma 4 is in Section A-D.

Following (89) , we evaluate the first factor of (101), $F^0[g,h]$, at $g = 0$ to obtain

$$F^0[0,h] = \exp\left(\left\langle\lambda_{k|k-1}, hf(\emptyset|\cdot)\right\rangle\right). \tag{103}$$

This is proportional to the PGFL of a PPP with intensity $\lambda_{k|k}(x) = f(\emptyset|x)\,\lambda_{k|k-1}(x)$, which proves (7).

We now need to compute the set derivatives in (102), evaluate them at $g = 0$ and compute the corresponding multi-object densities. For $V = \{v\}$ (set with a single element), we have

$$d_{\{v\}}[g,h] = \lambda^C(v) + \left\langle\lambda_{k|k-1}, h\frac{\delta}{\delta\{v\}}G[g|\cdot]\right\rangle \tag{104}$$

$$d_{\{v\}}[0,h] = \lambda^C(v) + \left\langle\lambda_{k|k-1}, hf(\{v\}|\cdot)\right\rangle \tag{105}$$

where we have applied the linear rule [3].

For $|V| > 1$, we have

$$d_V[g,h] = \left\langle\lambda_{k|k-1}, h\frac{\delta}{\delta V}G[g|\cdot]\right\rangle \tag{106}$$

$$d_V[0,h] = \left\langle\lambda_{k|k-1}, hf(V|\cdot)\right\rangle \tag{107}$$

where we have applied that the set derivative of a constant is zero. This is why the term $\lambda^C(v)$ is not present in (106).

The following lemma provides the form of the multi-object densities whose PGFL is $d_V[0,h]$ in (105) and (107).

Lemma 5. *The update of the PGFL of the PPP prior with measurement subset V*

$$w^V_{k|k}G^V_{k|k}[h] = d_V[g,h]\Big|_{g=0}$$

are PGFLs of weighted Bernoulli distributions with the form [11, Lem. 2]

$$f^V_{k|k}(X) = w^V_{k|k} \times \begin{cases} 1 - r^V_{k|k} & X = \emptyset \\ r^V_{k|k}f^V_{k|k}(x) & X = \{x\} \\ 0 & |X| > 1 \end{cases} \tag{108}$$

where

$$w^V_{k|k} = \left[\delta_1[|V|]\prod_{z\in V}\lambda^C(z)\right] + l^V_{k|k} \tag{109}$$

$$l^V_{k|k} = \left\langle\lambda_{k|k-1}, f(V|\cdot)\right\rangle \tag{110}$$

$$r^V_{k|k} = \frac{l^V_{k|k}}{w^V_{k|k}} \tag{111}$$

$$f^V_{k|k}(x) = \frac{f(V|x)\,\lambda_{k|k-1}(x)}{l^V_{k|k}}. \quad \square \tag{112}$$

Therefore, the PGFL of the updated PPP in (101) corresponds to the union of a PPP for undetected targets, with intensity $\lambda_{k|k}(x) = f(\emptyset|x)\,\lambda_{k|k-1}(x)$ and, a multi-Bernoulli mixture where each term in the mixture is a partition of W_0 and each Bernoulli component has a weight and density provided in Lemma 101. This concludes the proof of Theorem 1.

It should be noted that to perform the PMBM update we first take all possible sets $W_0 \uplus \cdots \uplus W_{n_{k|k-1}} = Z_k$, which represents subsets of Z_k associated to the PPP (W_0) or the previous Bernoullis (W_i, $i > 0$). Then, we take all possible partitions P of W_0, $P\angle W_0$, to generate the new Bernoulli components. A compact way to represent these decompositions is to take all possible subsets of Z_k to generate the new Bernoulli components and represent the possible data

associations to previous Bernoulli components, as in done in Theorem 1.

D. Set derivative of $F^0[g,h]$

We prove Lemma 4 by induction. The set derivative of $F^0[g,h]$, see (84), with respect to a set with $|W| = 1$ is straightforward, as there is a single partitioning of a one element set. For induction, we assume that the lemma holds up to a given size $|W|$, and we show that it holds for $\tilde{W} = W \cup \{z\}$:

$$\frac{\delta}{\delta \tilde{W}} F^0[g,h]$$

$$= \frac{\delta}{\delta\{z\}} \frac{\delta}{\delta W} F^0[g,h] \tag{113}$$

$$= \frac{\delta}{\delta\{z\}} \left(F^0[g,h] \sum_{P \angle W} \prod_{V \in P} d_V[g,h] \right) \tag{114}$$

$$= \left(\frac{\delta}{\delta\{z\}} F^0[g,h] \right) \sum_{P \angle W} \prod_{V \in P} d_V[g,h]$$

$$+ F^0[g,h] \sum_{P \angle W} \left(\frac{\delta}{\delta\{z\}} \prod_{V \in P} d_V[g,h] \right) \tag{115}$$

$$= F^0[g,h] d_{\{z\}}[g,h] \sum_{P \angle W} \prod_{V \in P} d_V[g,h]$$

$$+ F^0[g,h] \sum_{P \angle W} \sum_{V \in P} \left(\frac{\delta}{\delta\{z\}} d_V[g,h] \right) \prod_{V' \in P \setminus \{V\}} d_{V'}[g,h]. \tag{116}$$

Each step in the previous derivation results from the product rule [3].

From (102), we have $\frac{\partial}{\partial\{z\}} d_V[g,h] = d_{V \cup \{z\}}[g,h]$. In addition, each partitioning of $\tilde{W}$ consists of either a partitioning of W with an additional single element subset $\{z\}$; or a partitioning of W, adding element z to one of the existing subsets [3, App. D.2]. Since the top line in (116) handles the former case and the bottom line handles the latter case, we find that (116) is equivalent to $F^0[g,h] \sum_{P \angle \tilde{W}} \prod_{V \in P} d_V[g,h]$, which proves Lemma 4.

APPENDIX B

A. Single-target integral

Given a real-valued function $\pi(\cdot)$ on $\mathcal{X} = \mathbb{R}^{n_x} \uplus \mathcal{X}_e$ such that

$$\pi(x) = \begin{cases} \pi_p(x) & x \in \mathbb{R}^{n_x} \\ \pi_e(\gamma, \xi, X) & x = (\gamma, \xi, X) \in \mathcal{X}_e, \end{cases} \tag{117}$$

its single target-integral is the sum of the integrals in $\mathbb{R}^{n_x}$ and $\mathcal{X}_e$ [3, Sec. 3.5.3]

$$\int_{\mathcal{X}} \pi(x)\, dx = \int_{\mathbb{R}^{n_x}} \pi_p(x)\, dx + \int_{\mathbb{S}_+^d} \int_{\mathbb{R}^{n_x}} \int_{\mathbb{R}_+} \pi_e(\gamma, \xi, X)\, d\gamma d\xi dX. \tag{118}$$

TABLE II: Update and marginal likelihood of a GGIW density

Input: Prior GGIW parameters $\zeta_+ = (\alpha_+, \beta_+, \overline{x}_+, P_+, v_+, V_+)$, set W of measurements.
Output: $(\zeta, \ell) = \mathrm{u}_e(\zeta_+, W)$, where ζ are the updated GGIW parameters and ℓ the marginal likelihood evaluated at W.

If $|W| > 0$

$$\zeta = \begin{cases} \alpha &= \alpha_+ + |W| \\ \beta &= \beta_+ + 1 \\ \overline{x} &= \overline{x}_+ + K\varepsilon \\ P &= P_+ - KHP_+ \\ v &= v_+ + |W| \\ V &= V_+ + N + Z \end{cases}$$

where

$$\overline{z} = \frac{1}{|W|} \sum_{z \in W} z$$

$$Z = \sum_{z \in W} (z - \overline{z})(z - \overline{z})^T$$

$$\hat{X} = V_+ (v_+ - 2d - 2)^{-1}$$

$$\varepsilon = \overline{z} - H\overline{x}_+$$

$$S = HP_+H^T + \frac{\hat{X}}{|W|}$$

$$K = P_+H^T S^{-1}$$

$$N = \hat{X}^{1/2} S^{-1/2} \varepsilon\varepsilon^T S^{-T/2} \hat{X}^{T/2}$$

$$\ell = \left(\pi^{|W|}|W|\right)^{-d/2} \frac{|V_+|^{\frac{v_+ - d - 1}{2}} \Gamma_d\left(\frac{v - d - 1}{2}\right) \left|\hat{X}\right|^{1/2} \Gamma(\alpha) (\beta_+)^{\alpha_+}}{|V|^{\frac{v-d-1}{2}} \Gamma_d\left(\frac{v_+ - d - 1}{2}\right) |S|^{1/2} \Gamma(\alpha_+) (\beta)^{\alpha}}.$$

If $|W| = 0$

$$\zeta = (\alpha_+, \beta_+ + 1, \overline{x}_+, P_+, v_+, V_+)$$

$$\ell = \left(\frac{\beta_+}{\beta_+ + 1}\right)^{\alpha_+}.$$

B. Relation to spaces in interacting multiple models

We explicitly relate the space of coexisting point extended targets, $\mathcal{X} = \mathbb{R}^{n_x} \uplus \mathcal{X}_e$, in Section IV to spaces used in interacting multiple models [29], which usually include a class variable to distinguish between different models. Given $x \in \mathbb{R}^{n_x} \uplus \mathcal{X}_e$, we know if x represents a point target or an extended target as $\mathbb{R}^{n_x}$ and $\mathcal{X}_e$ are disjoint. Therefore, it is not necessary to extend the single target space with a class variable to distinguish both types of targets.

Nevertheless, it is possible to add a class variable c such that the single target state becomes $y = (c, x)$, where $c = 0$ for point targets and $c = 1$ to extended targets. In this case, the single target space is $(\{0\} \times \mathbb{R}^{n_x}) \uplus (\{1\} \times \mathcal{X}_e)$ and the PMBM filtering recursion remains unchanged.

APPENDIX C

For completeness, in this appendix, we provide the (approximate) single extended target update for factorised GGIW priors [5], [30]. The resulting expressions are provided in Table II. The update for the parameters of the Gamma distribution is exact due to the Poisson-Gamma conjugacy.